

¹²C. M. Lederer, J. M. Hollander, and I. Perlman, *Table of Isotopes* (John Wiley & Sons, New York, 1967).

¹³L. S. Kisslinger and Chi-Shiang Wu, *Phys. Rev.* **136**, B1254 (1964).

¹⁴P. W. M. Glaudemans, P. J. Brussaard, and B. H. Wildenthal, *Nucl. Phys.* **A102**, 593 (1967).

¹⁵J. B. French, E. C. Halbert, J. B. McGrory, and

S. S. M. Wong, in *Advances in Nuclear Physics*, edited by M. Baranger and E. Vogt (Plenum Press, Inc., New York, 1969) Vol. 3, pp. 193–257.

¹⁶B. H. Wildenthal, *Phys. Rev. Letters* **22**, 1118 (1969).

¹⁷J. Kern, G. L. Struble, and R. K. Sheline, *Phys. Rev.* **153**, 1331 (1967).

Collective States in the $N = 82$ Nuclide ^{141}Pr Excited by the (α, α') Reaction at 45 MeV*

Helmut W. Baer,[†] Henry C. Griffin, and W. S. Gray

Cyclotron Laboratory, The University of Michigan, Ann Arbor, Michigan 48105

(Received 22 July 1970)

The $^{141}\text{Pr}(\alpha, \alpha')$ reaction at $E_{\alpha} = 45.0$ MeV and $\Delta E_{\alpha'} \approx 35$ keV was studied to investigate the particle-vibration interaction in this $N = 82$ nuclide and to elucidate the ^{141}Pr level structure in the 0–4-MeV region. The α -particle angular distributions were measured in $\leq 2^\circ$ steps over ranges of 7 – 80° for elastic scattering and 12 – 66° for inelastic scattering. A $^{141}\text{Pr}(d, d')$ spectrum at $E_d = 28.7$ MeV and with higher resolution (20 keV) was also recorded. These measurements, in combination with other high-resolution studies, establish the existence of approximately 50 levels with excitation energies of 1.1–3.0 MeV. Approximately 20 of these levels can be identified in the (α, α') spectra and are interpreted as states with significant collective components. Although most of these levels are in either a positive-parity group between 1.1 and 1.9 MeV or a negative-parity group between 2.0 and 2.5 MeV, it is found that the assumption of a weak particle-vibration interaction based on the 2^+ and 3^- core states of ^{140}Ce and the $d_{5/2}$ ground state of ^{141}Pr is inadequate to explain the results. Qualitative agreement is found with the results of recent shell-model studies which assumed nine active protons outside an inert $Z = 50$, $N = 82$ core. In addition, some evidence is found for the approximate validity of the $\Delta B = 0$ selection rule for inelastic scattering transitions which was recently proposed by Hecht and Adler.

I. INTRODUCTION

In recent years there has been considerable interest in the study of $N = 82$ nuclei. This interest has been stimulated largely by the hope that the properties of most of the low-lying levels can be described in terms of configurations involving only the protons outside the $Z = 50$ core. The success of the recent shell-model studies performed by Wildenthal,¹ Hecht and Adler,² and Jones *et al.*³ has shown that this assumption provides a reasonable basis for describing some properties of $N = 82$ nuclei. These calculations, which take into account only positive-parity proton excitations, are able to reproduce the main features of the observed excitation spectra up to approximately 2.5 MeV. Moreover, they are in moderately good agreement with the spectroscopic information which has been obtained from recent proton-transfer experiments using the $(d, {}^3\text{He})$, (t, α) , and $({}^3\text{He}, d)$ reactions, which have now been performed for each of the seven stable $N = 82$ targets.^{3–9}

There were, however, questions which were

not resolved by the existing experiments. In the $({}^3\text{He}, d)$ experiments, for example, a single $l = 5$ transition was reported for each of the even- A targets, but with a spectroscopic factor closer to 0.7 than the value near unity expected if the $1h_{11/2}$ proton state is a pure one-quasiparticle (1-qp) state. The reduction in the $l = 5$ spectroscopic strength could be understood if, as has been suggested by Ellegaard *et al.*⁷ in the case of ^{141}Pr , the $1h_{11/2}$ 1-qp state mixes strongly with a particle-vibration state based on the coupling of the $2d_{5/2}$ 1-qp state with an octupole vibration of the ^{140}Ce core. While this explanation appeared plausible, there had been no quantitative measurements of the extent of particle-vibration coupling in the $N = 82$ nuclei.

The more general question of the role played by collective excitations in the $N = 82$ nuclei has been little studied. It is known that a collective 3^- state exists at about 2–3 MeV in the even- A nuclei. In ^{140}Ce the 3^- state is at 2.464 MeV and is highly collective.^{10, 11} Also the $B(E2)$ value measured for the first 2^+ state at 1.597 MeV in ^{140}Ce

is 16 times the Weisskopf estimate.¹² In the neighboring odd-mass nucleus ^{141}Pr , therefore, one might reasonably expect to find particle-vibration multiplets arising from the coupling of the 1-qp proton states with quadrupole and octupole vibrations of the ^{140}Ce core. However, one does not expect the simple picture of the weak-coupling model to hold for a nucleus like ^{141}Pr . Within a few hundred keV of the 2^+ state at 1.6 MeV in ^{140}Ce there are states having $J^\pi = 0^+, 4^+, \text{ and } 6^+$, and there is also a 5^- state located within approximately 100 keV of the 2.46-MeV 3^- state.^{10, 13} Based upon these additional core excitations one can construct many additional states in ^{141}Pr and one expects considerable mixing between these states and the "pure" particle-vibration states.

It is well known that α -particle scattering preferentially excites collective states and can lead to reliable spin-parity information. Recently the structure of ^{140}Ce has been studied with this reaction by Baker and Tickle.¹¹ The purpose of the present $^{141}\text{Pr}(\alpha, \alpha')$ experiment was to identify the levels in the ^{141}Pr spectrum having significant particle-vibration components and if possible to relate them to the ^{140}Ce core states. In addition it was thought desirable for the purpose of evaluating the results of recent shell-model studies^{1, 2} to obtain more information on the distribution of positive- and negative-parity states in the 1–3-MeV excitation region of ^{141}Pr .

During the course of the experiment a selection rule for inelastic scattering transitions was proposed by Hecht and Adler.² This selection rule is based upon the pseudospin quantum number B , a generalization of the seniority quantum number which reflects the correlated motion of $J \neq 0$ pairs. These authors have shown that under suitable assumptions only inelastic transitions having $\Delta B = 0$ are allowed. In view of the fact that both $\Delta B = 0$ and $\Delta B = 1$ transitions might be expected in the $^{141}\text{Pr}(\alpha, \alpha')$ reaction, it was of considerable interest in the present study to test the validity of this selection rule.

II. EXPERIMENTAL PROCEDURES AND RESULTS

All of the measurements were performed with a single target of ^{141}Pr . This target was prepared by evaporating praseodymium metal from a tantalum boat into a $\approx 50\text{-}\mu\text{g cm}^{-2}$ carbon film. To minimize oxidation and changes in the target thickness from sputtering, a $\approx 10\text{-}\mu\text{g cm}^{-2}$ layer of carbon was evaporated onto the Pr foil. The target thickness (0.40 mg cm^{-2} Pr) was deduced by measuring the energy loss of ^{241}Am α particles and by comparing elastic scattering yields, over the

range 7 to 36° , with optical-model predictions based on the parameters of Ref. 14. The major sources of uncertainty in the thickness are possible variations in target positioning and in beam conditions (which would vary the exposed portion of the target) and possible changes in the target thickness over the course of the measurements. However these uncertainties were not evaluated independent of others, such as uncertainties in track counting and effective solid angle. The overall experimental uncertainties were 10–15% and are discussed in Sec. IV B.

The α -particle inelastic scattering measurements were made with 45.0-MeV $^4\text{He}^{2+}$ ions from the University of Michigan 83-in. cyclotron.¹⁵ Beam currents were typically 0.1 to 0.2 μA at an energy spread of approximately 20 keV. Beam exposures were determined with a Faraday cup and a current integrator. Scattered particles were analyzed with a 180° , $n = \frac{1}{2}$ magnetic spectrograph and were detected in Ilford K0 nuclear emulsion plates. An example of a relatively good α -particle spectrum is shown in Fig. 1.

Although the linewidths obtained for the α -particle spectra were 30–35 keV, it can be seen from Fig. 1 that this resolution was insufficient to resolve all of the levels with excitation energies below 4 MeV. In order to further resolve individual levels in this region and to obtain more accurate excitation energies, an additional higher-resolution $^{141}\text{Pr}(d, d')$ spectrum was recorded. This spectrum had linewidths of 20 keV and is shown in Fig. 2. All of the levels below 3.135 MeV which are resolved in the (α, α') spectra can be identified in the (d, d') spectrum, and no significant differences in relative intensities are observed other than those which can be associated with differences in the phases of the angular distributions for odd- and even- L transfers. Therefore, the excitation energies of the levels up to 3.135 MeV were determined from the higher-resolution deuteron spectrum. The energy calibration was determined by comparing deuteron spectra of ^{141}Pr and ^{140}Ce taken at the same spectrograph field setting. Transitions to levels at 1.597, 2.084, 2.464, and 2.900 MeV¹³ in ^{140}Ce were used as calibration points. The estimated uncertainties of the energies of levels up to 3.135 MeV are 10 keV. The energies of levels above 3.135 MeV were obtained by energy extrapolation in the (α, α') spectra. These energies are estimated to have uncertainties of about 20 keV. The energy values determined in the present work are listed in columns 1 and 2 of Table I.

Angular distributions for 16 inelastic α -particle groups (see Figs. 5–10) were obtained from spectra similar to Fig. 1, taken at 30 scattering angles

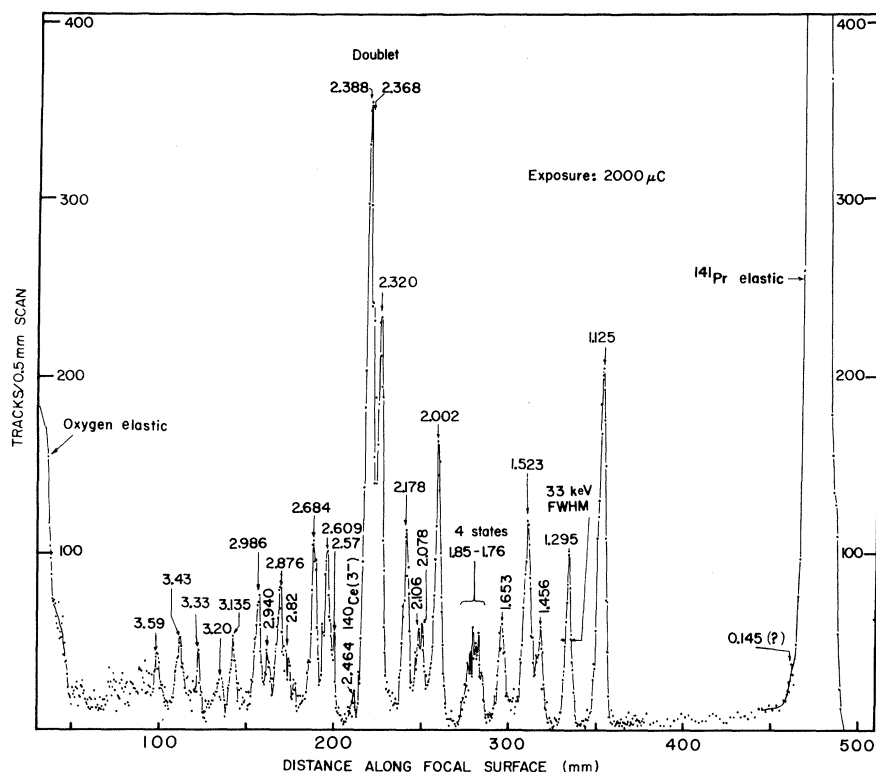


FIG. 1. Spectrum of α particles scattered from ^{141}Pr at 40° (lab). The peaks are labeled with the corresponding excitation energies in MeV.

(center-of-mass angles of 12.2 to 65.9°). Exposures for these spectra ranged from 0.2 mC for the small angles to 3 mC for large angles. The angular convergence of the incident beam was limited to 1.2° by apertures in the beam preparation system. The magnetic spectrograph accepted a total of 2° in the reaction plane and could be positioned relative to the scattering chamber coordinates with an uncertainty of less than 0.1° . The zero scattering angle was determined by comparing elastic scattering yields on both sides of the beam direction. On the basis of several determinations of this quantity at different times and under different cyclotron tuning conditions, we estimate that the uncertainty in the scattering angle due to variations in the incident beam did not exceed 0.2° .

The differential cross sections were calculated from peak areas, which were obtained from the number of tracks (corrected for background) observed in a region of a spectrum of approximately twice the average full width at half maximum (FWHM) for that spectrum. A larger range of integration was used for some groups of levels, and a smaller range was used to handle some closely spaced groups. The presence of oxygen and carbon in the target eliminated several points from each angular distribution. The error bar shown with each datum in the angular distributions re-

flects the statistical uncertainty (standard deviation) in the net area of the corresponding spectral peak. An additional uncertainty is due to possible plate reading errors, since variations as large as 10% were observed when different scanners read the same plate. Spectra for several scattering angles in the range 30 – 45° were repeated during the course of the measurements. Differences in differential cross sections at a given angle obtained from these spectra indicate that nonstatistical uncertainties are 10 – 15% .

The elastic scattering angular distribution was obtained in a manner similar to that used for inelastic scattering, except that the acceptance angle of the analyzing magnet was $\leq 1^\circ$ and the scattered particles were detected with a position-sensitive detector placed in the image surface of the magnetic spectrograph. Data were obtained for 41 center-of-mass scattering angles in the range 7.2 – 79.4° . These results are given in Fig. 3 and Table II. Data obtained with the nuclear emulsions for elastic scattering at large angles are in good agreement with these results.

The high density of levels above 1.1 MeV in ^{141}Pr makes it difficult in many cases to establish with certainty whether a given spectral peak corresponds to a single transition or to several transitions to close-lying levels. Based on the experimental results obtained in this work, one

TABLE I. Summary of data on excitation energies and J^π values for levels of ^{141}Pr including results of present work and other recent experiments. In each column are listed the measured excitation energies (MeV) and J^π values when determined. A value in parentheses is regarded as tentative by the original investigators. At the top of each column the type of experiment is identified and approximate resolution FWHM values are given. The bombarding energies for the charged-particle reaction experiments are also given.

Present	Ellegaard <i>et al.</i> (d, d') $E = 12 \text{ MeV}$ $\sim 10 \text{ keV}$ (Ref. c)	van der Merwe <i>et al.</i> ($n, n'\gamma$) Ge(Li) $\sim 10 \text{ keV}$	Dave, Nelson, and Wilenzick ($n, n'\gamma$) Ge(Li) $\sim 3 \text{ keV}$	Moreh and Nof (γ, γ') Ge(Li)	Wildenthal <i>et al.</i> ($^3\text{He}, d$) $E = 40 \text{ MeV}$ $\sim 35 \text{ keV}$	Beery, Kelley, and McHarris β^+, EC Ge(Li) $\sim 5 \text{ keV}$	Collation of results
0.15	0.147	0.145	0.145	0.145	0.145 $\frac{7}{2}^+$	0.1454 $\frac{7}{2}^+$	0.145 ^c $\frac{7}{2}^+$
1.125 ^d	1.122	1.118	1.118	1.130 $\frac{3}{2}^+$	1.11 $\frac{11}{2}^-$	1.1268 $(\frac{3}{2}^+)$	1.118 $\frac{11}{2}^-$
1.295	1.296	1.293	1.228	1.293		1.2925 $(\frac{5}{2}^+)$	1.127 $\frac{3}{2}^+$
			1.292			1.2984 $(\frac{1}{2}^+ - \frac{5}{2}^+)$	1.293 $\frac{5}{2}^+$
			1.299		1.30 $\frac{1}{2}^+$		1.298 $\frac{1}{2}^+$
1.456	1.437	1.436	1.435	1.437 $\frac{3}{2}^+$			1.437 $\frac{3}{2}^+$
			1.450	1.451 $(\frac{3}{2}^+, \frac{7}{2}^+)$			1.452
			1.456				1.456 +
			1.493				1.493
1.523	1.525	1.521	1.520	(1.512)			(1.512)
	1.584	1.578	1.578	1.582			1.521 $(\frac{3}{2}^+)^+$
	1.609	1.607	1.607			1.5800 $(\frac{5}{2}^+)$	1.580 $(\frac{5}{2}^+)$
1.653	1.652	1.650	1.649	(1.650)	1.60 $\frac{3}{2}^+$	1.6079 $(\frac{1}{2}^+ - \frac{5}{2}^+)$	1.608 $\frac{3}{2}^+$
					1.65 $\frac{1}{2}^+$		1.650 $\frac{1}{2}^+$
1.764	1.764					1.6572 $(\frac{1}{2}^+ - \frac{5}{2}^+)$	1.657
		(1.695)					(1.695)
		(1.705)					(1.705)
1.792	1.799	1.782	1.783				1.764
1.812	1.817	1.808	1.809				1.783
1.848	1.849	1.844	1.841	1.847			1.809
							1.823
							1.844
	Unresolved						
	group of						
	states						

TABLE I (Continued)

Present	Ellegaard <i>et al.</i> (d, d') $E = 12$ MeV ~ 10 keV (Ref. c)	van der Merwe <i>et al.</i> ($\alpha, n^*\gamma$) Ge(Li) ~ 10 keV	Dave, Nelson, and Wilenzick ($\alpha, n^*\gamma$) Ge(Li) ~ 3 keV	Moreh and Nof (γ, γ') Ge(Li)	Wildenthal <i>et al.</i> ($^3\text{He}, d$) $E = 40$ MeV ~ 35 keV	Beery, Kelley, and McHarris β^+, EC Ge(Li) ~ 5 keV	Collation of results
			1.856				1.856
			(1.900)				(1.900)
2.002	2.002-	2.004	1.974				1.974
2.078	2.078-	2.079	2.016	2.016			2.003 - 2.016 2.079 -
2.106	2.106-	2.107					2.107 -
2.178	2.178-	2.176	2.104				2.177 -
2.256	2.256+			2.235 $\frac{3}{2}^{(+)}$			2.235 $\frac{3}{2}^{(+)}$ 2.256 + 2.272
2.320	2.320-	2.319		2.272			2.320 -
2.368	2.368-	2.364		2.348			2.348 2.368 -
2.388	2.388-	2.386					2.388 - (2.480)
2.57	2.57	2.566		2.524			2.524 2.566
2.609	2.609+	2.585		2.566			2.589
2.684	2.684-	2.607		2.589			2.608 + 2.681 -
(2.730)				(2.700)			(2.700) (2.730)
			2.791				2.791

TABLE I (Continued)

Present (d, d') $E = 29$ MeV ~ 20 keV (Ref. a)	(α, α') $E = 45$ MeV ~ 35 keV (Ref. b)	Ellegaard <i>et al.</i> (d, d') $E = 12$ MeV ~ 10 keV (Ref. c)	van der Merwe <i>et al.</i> ($n, n'\gamma$) Ge(Li) ~ 10 keV	Dave, Nelson, and Wilenzick ($n, n'\gamma$) Ge(Li) ~ 3 keV	Moreh and Nof <i>et al.</i> (γ, γ') Ge(Li)	Wildenthal <i>et al.</i> ($^3\text{He}, d$) $E = 40$ MeV ~ 35 keV	Beery, Kelley, and McHarris β^+, EC Ge(Li) ~ 5 keV	Collation of results
2.820	2.820	2.813						2.813
2.843		2.843						2.843
2.876	2.876	2.868						2.868
2.940	2.940	2.930						2.936
2.986	2.986+							2.986 +
3.135	3.135							3.135
	3.20							3.20
	3.33							3.33
	3.43							3.43
	3.59							3.59

^aUncertainties are ± 10 keV with the exception of the state at 2.57 ± 0.02 MeV.

^bAll states up to 3.135 MeV observed in the (α, α') spectrum were also observed in the (d, d') spectrum, therefore energy values were obtained from the higher-resolution (d, d') data (column 1). States above 3.135 MeV were observed only in the (α, α') spectrum and energy uncertainties for these states are ± 20 keV.

^cUncertainties are ± 10 keV.

^dUnresolved doublet; the angular distribution of the $^{141}\text{Pr}(\alpha, \alpha')$ differential cross section indicates the presence of a positive- and negative-parity component.

^eA value 145.450 ± 0.005 keV was determined by use of a curved-crystal spectrometer (see Ref. 8).

sphere of radius $R_C = r_C A^{1/3}$. The parameter values which were employed are $V_r = 151.0$ MeV, $V_{im} = 19.2$ MeV, $r_o = 1.404$ F, $a = 0.555$ F, and $r_C = 1.30$ F. These values, quoted by Jackson and Morgan,¹⁴ were obtained from an analysis of the elastic scattering of α particles from ^{140}Ce at 42–44 MeV. It can be seen from Fig. 3 that this potential provides a reasonably good description of elastic scattering from ^{141}Pr in the angular range covered by the data. It was therefore employed in the distorted-wave Born-approximation (DWBA) analysis of the inelastic scattering angular distributions.

B. Form Factor and Cross Sections Based on the Collective Model

The calculation of the DWBA transition amplitude was based upon a conventional interaction model in which the projectile induces a one-step transition in the target to vibrational states described by a collective-model Hamiltonian. Refinements on this model, such as explicit treatment of channel coupling and nonlocality, were not included. The application of the model to inelastic α -particle scattering has been discussed in detail by Bassel *et al.*¹⁸ and Rost.¹⁹ In brief, the interaction of the α particle with the nucleus is described in terms of a nonspherical optical-model potential whose shape oscillates about a spherical mean. In the context of first-order perturbation theory, inelastic scattering leading to the collective vibrations is induced by the nonspherical part of the potential. A Taylor series expansion of the potential about the mean radius R gives a first-order interaction term of the form¹⁸

$$V_{LM} = i^L R [dU(r-R)/dr] \alpha_{LM}^*, \quad (2)$$

where $U(r-R)$ is the spherical optical-model potential with geometric parameters R and a . In the quantal interpretation of the first-order term the deformation parameters α_{LM}^* are regarded as dynamical variables able to create or annihilate phonons with angular momentum L and Z component M . For an even- A nucleus with no phonons present in the ground state the first-order interaction can excite a single 2^L -pole phonon, leading to a final nuclear state with spin $J=L$ and parity $(-1)^L$. The reduced matrix element connecting the initial and final nuclear states then has the value

$$\begin{aligned} \langle J=L \| V_L \| J_i=0 \rangle &= -i^L R \frac{dU}{dr} \left(\frac{\hbar\omega_L}{2C_L} \right)^{1/2} \\ &= -i^L F(r) \beta_L (2L+1)^{-1/2}, \quad (3) \end{aligned}$$

where $\beta_L = [(2L+1)(\hbar\omega_L/2C_L)]^{1/2}$ and C_L is the restoring-force parameter. The radial form factor $F(r) = R(dU/dr)$ is uniquely determined by the optical-model potential which describes the elastic scattering. The deformation parameter β_L is the only unspecified quantity and it is to be extracted from a comparison with the measured cross sections.

The inelastic scattering cross section which follows from this description of the scattering event has been calculated in the DWBA by Bassel *et al.*¹⁸ For an even- A nucleus the cross section for excitation of a state with spin $J=L$ can be reduced to the form

$$\frac{d\sigma}{d\Omega} (0 \rightarrow L) = \beta_L^2 \sigma_L(\theta), \quad (4)$$

in which the normalization of the reduced cross section $\sigma_L(\theta)$ is determined by the choice of optical-potential parameters.

In the collective vibrational model of odd- A nuclei, multiplets of levels may be formed by the coupling of the extra nucleon to the phonon (core) states of the neighboring even nucleus. If one assumes that the wave functions for these multiplets are simply the vector-coupled product of the phonon state and the single-particle state, the inelastic scattering cross section to each member

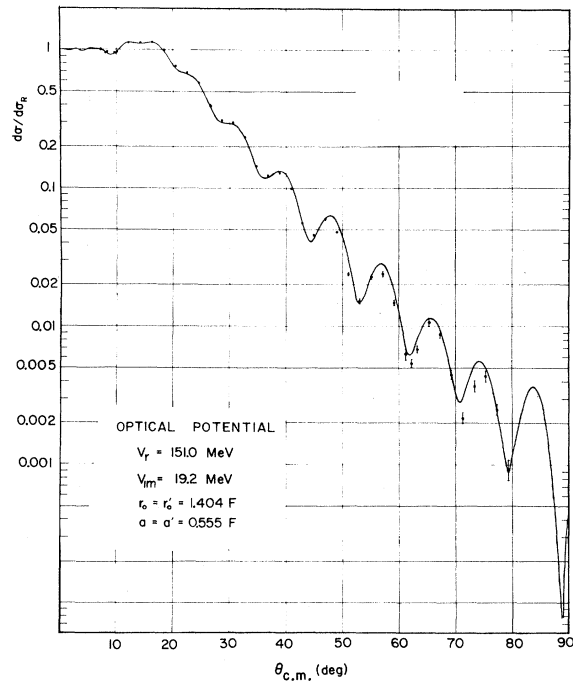


FIG. 3. Angular distribution for elastic scattering of 45.0-MeV α particles from ^{141}Pr . The solid curve is the optical-model prediction given by the potential parameters shown in the figure.

of the multiplet is related to the core-state cross section by^{20,21}

$$\frac{d\sigma}{d\Omega}(J_i \rightarrow J) = \frac{2J+1}{(2J_i+1)(2L+1)} \frac{d\sigma}{d\Omega}(0 \rightarrow L) \\ = [\beta_L^P(J)]^2 \sigma_L(\theta), \quad (5)$$

where J_i and J are the initial and final nuclear spins, and conservation of angular momentum requires $\vec{J} = \vec{J}_i + \vec{L}$. In this "weak-coupling" model, the partial deformation parameters $\beta_L^P(J)$ are related to the core deformation parameter β_L by²¹

$$\beta_L^P(J) = \left[\frac{2J+1}{(2J_i+1)(2L+1)} \right]^{1/2} \beta_L, \quad (6)$$

and

$$\sum_J [\beta_L^P(J)]^2 = \beta_L^2, \quad (7)$$

where the sum ranges over the possible J values of the multiplet, given by

$$|L - J_i| \leq J \leq L + J_i.$$

The relationship (5) between the cross sections will be violated when the pure particle-vibration multiplets mix with other configurations. This is likely to occur in most odd- A nuclei and is the case for ^{141}Pr . In these circumstances the partial deformation parameters can be regarded as a simple means of parametrizing the reaction cross sections. However, a value of $\beta_L^P(J)$ extracted from an experimental angular distribution can always be related to the nuclear wave functions. The definition of the partial deformation parameter in terms of the nuclear matrix elements is²¹

$$\beta_L^P = (2L+1)^{1/2} \langle J || \alpha_L^* || J_i \rangle, \quad (8)$$

in which the initial and final states are not restricted to the simple vector-coupled states of the weak-coupling model.

The reduced cross sections $\sigma_L(\theta)$ were calculated with the DWBA code DWUCK.²² The optical-model potential parameters employed were given in Sec. III A. The contributions to inelastic scattering from the absorptive part of the potential were neglected. The only effect of including the imaginary term in the form factor would be to increase the calculated reduced cross sections by a factor of $[1 + (W/V)^2]$, which has a value 1.016 for the four-parameter potential used in present analysis. The resulting change in the extracted values of $\beta_L^P(J)$ would therefore be less than 1%.

C. Coulomb Excitation

Bassel *et al.*¹⁸ have shown that the presence of the Coulomb force can have a considerable effect

upon the calculated inelastic angular distributions at forward angles. Baker and Tickle¹¹ recently have measured the differential cross sections for inelastic scattering of 45-MeV α particles to the 2^+ and 3^- states in ^{140}Ce and the 3^- state in ^{208}Pb . This investigation shows that the shapes of these angular distributions at forward angles are quite sensitive to the interference between Coulomb and nuclear scattering and that this effect is well described by the procedure discussed by Bassel *et al.*¹⁸ Since our data extend inward to 12° , we included the effect of Coulomb excitation in the present calculations. With the assumption that the optical potential and charge density undergo the same deformation, the effect of Coulomb excitation may be taken into account¹⁸ by the addition of a term

$$C_L(r) = 3.0ZZ'e^2(2L+1)^{-1}R_C^L r^{-(L+1)}, \quad r \geq R_C \\ = 0, \quad r < R_C, \quad (9)$$

to the nuclear form factor. According to the discussion given by Bassel *et al.*¹⁸ one can expect the effect of Coulomb excitation to be taken into account accurately at angles larger than the classical deflection angle, $\theta_c = 2\eta/L$. For the scattering of 45-MeV α particles by ^{141}Pr , for which $\eta = 5.54$, θ_c has the value 6.3° for $L = 101$. Since the code DWUCK has provision for the inclusion of up to 102 partial waves, we expect the calculations to be adequate over the range covered by the data.

An additional consideration is the value of the upper cutoff for the radial integrals. The values of angular momentum omitted by such a cutoff correspond classically¹⁸ to $L \geq [KR_{\max}(KR_{\max} - 2\eta)]^{1/2}$. In the present analysis the radial integrals were carried out to 40 F with a step size of 0.1 F. For 45-MeV α particles incident upon ^{141}Pr the value 40 F corresponds classically to $L = 108$. Therefore, we expect the cutoff of 40 F to be adequate for the calculations, which included 102 partial waves.

Comparisons of reduced cross sections $\sigma_L(\theta)$ for $L = 2$ and $L = 3$ transitions, with and without the inclusion of Coulomb excitation (C.E.), are shown in Fig. 4. The value $R_C = 1.2A^{1/3}$ was used in the form factor. The $L = 2$ angular distribution is modified considerably by the inclusion of C.E. The number of partial waves for the $L = 2$ curves displayed in the figure is 102. However, the differences between the calculations employing 80 and 102 partial waves were quite small at all angles. The effect of including C.E. in an $L = 3$ transition is seen (Fig. 4) to be much less than for the $L = 2$ transition. The smaller effect of C.E. upon an $L = 3$ transition can be understood from

the fact that the C.E. form factor for the transfer of three units of angular momentum falls off as r^{-4} outside the nuclear charge distribution, as compared to r^{-3} for two units of angular momentum transfer.

IV. DISCUSSION

A. Comparison of Results with Those of Other Experiments

The energy values determined in the present work are listed in columns 1 and 2 of Table I. Also listed in the table are the results of several other recent high-resolution experiments. These include the decay-scheme study of Beery, Kelley, and McHarris,²³ the $(n, n'\gamma)$ experiments of van der Merwe, van Heerden, McMurray, and Malan,²⁴ Dave, Nelson, and Wilenzick,²⁵ and the (γ, γ') study of Moreh and Nof.²⁶ In column 9 we have combined the results of the various experiments and have listed the most accurate values of the excitation energies. (In a few cases an average value is given.) Also shown are spin-parity values for the levels where these have been measured.

It can be seen in Fig. 2 that the first excited state of ^{141}Pr at 0.145 MeV is populated very weakly in the (d, d') reaction. In the (α, α') spectrum (Fig. 1) the transition to this level is obscured by the intense elastic scattering peak and appears only as a possible shoulder on the low-energy side of the peak. Although some structure is discernable in the low and essentially continuous background appearing in each spectrum between 0.145 and 1.125 MeV, no additional levels could be identified in this region. The structure which does appear most likely consists of kinematically broadened groups due to scattering from light impurities in the target. All of the experiments are consistent with the conclusion that, other than the ground state and the 0.145-MeV level, there are no levels in ^{141}Pr below 1.1 MeV.

To facilitate the discussion of experimental results, it is convenient to divide the remaining levels into energy regions corresponding to predominantly odd- L and even- L transfer. For example, the inelastic scattering distributions for the four strong transitions leading to levels at 1.295, 1.456, 1.523, and 1.653 MeV (see Fig. 5) are out of phase with the elastic scattering angular distribution (Fig. 3). In view of the fact that the excitation energies of these four levels are approximately those of the one-phonon 2^+ states in ^{140}Ce (1.60 MeV) and ^{142}Nd (1.57 MeV), we expect a one-step excitation process to dominate and expect the Blair phase rule²⁰ to be valid. Therefore, these transitions are of even L and lead to positive-

parity states. Most of the transitions to levels in the region of 1.12–1.85 MeV show similar angular patterns and imply even- L transfer. The second energy region includes levels between 2.0 and 2.5 MeV, where most of the transitions show odd- L character. Finally, transitions to levels above 2.5 MeV are generally weaker, cannot be grouped according to parity, and have been studied by at most two of the other experiments summarized in

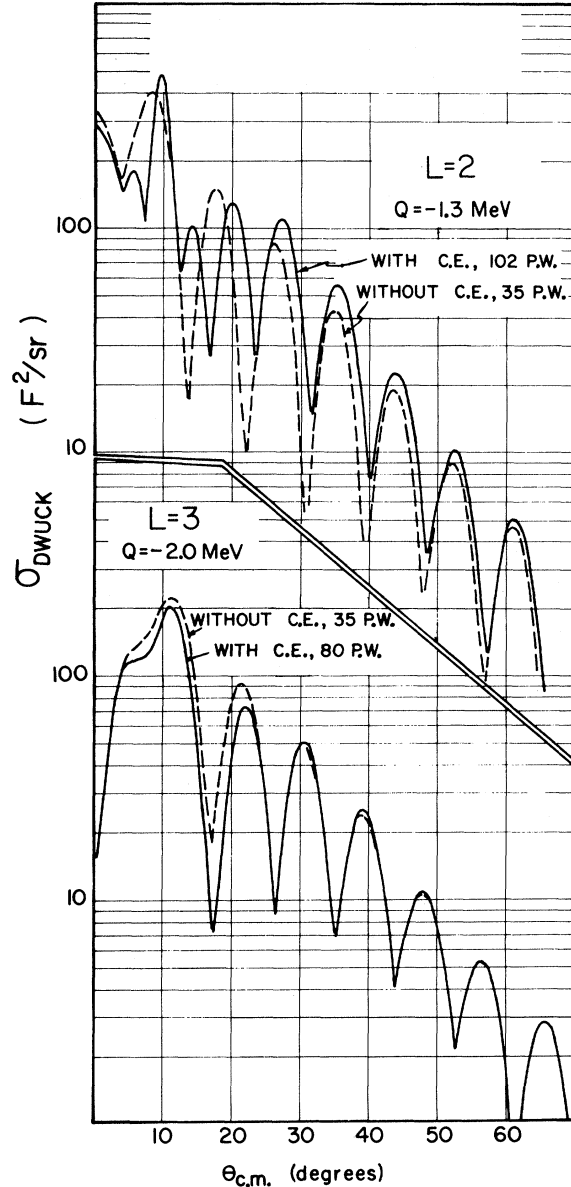


FIG. 4. A comparison of DWBA predictions for $L=2$ and $L=3$ transitions with and without the inclusion of Coulomb excitation (C.E.). The calculations were performed with the number of particle waves (P.W.) indicated in the figure. The partial deformation lengths ($\beta_{L,R}^2$) are defined in the text.

Table I. These transitions are discussed briefly as the third group.

1. *Positive-Parity Multiplet, 1.12–1.86 MeV*

The excitation energies determined in the present experiment are in very good agreement with those determined by Ellegaard *et al.*⁷ in a study of the $^{141}\text{Pr}(d, d')$ reaction at $E_d = 12$ MeV. In the region 1.437–1.653 MeV, strong transitions to levels at 1.456, 1.523, and 1.653 MeV are observed in both experiments. In addition, weaker transitions to levels at 1.437, 1.498, 1.584, and 1.609 MeV were resolved in the higher-resolution spectra of Ellegaard *et al.* The latter four levels and an additional level at 1.450 MeV were observed in $^{141}\text{Pr}(n, n'\gamma)$ experiments.^{24,25} Four levels between 1.764 and 1.848 MeV were resolved both in the present (d, d') spectrum and in the (d, d') work of Ellegaard *et al.* The two $^{141}\text{Pr}(n, n'\gamma)$ experiments^{24,25} each indicated the presence of four levels in this region although not the same four levels. Van der Merwe *et al.*²⁴ report a level at 1.823 MeV which was not reported by Dave, Nelson, and Wilenzick,²⁵ while the latter authors reported a level at 1.856 MeV not reported by van der Merwe *et al.* A comparison of all the experimental results suggests the existence of levels at 1.764, 1.783, 1.809, 1.823, 1.844, and 1.856 MeV.

A strong $l = 5$ transition was observed^{4,5} in the $^{140}\text{Ce}(^3\text{He}, d)^{141}\text{Pr}$ reaction to a level at 1.11 MeV. This level has been interpreted as the $1h_{11/2}$ qp state.⁸ Another level at 1.127 MeV was observed²³ in the decay $^{141}\text{Nd} \rightarrow ^{141}\text{Pr}$, the $^{141}\text{Pr}(n, n'\gamma)$ studies,^{24,25} and the $^{141}\text{Pr}(\gamma, \gamma')$ study.²⁶ A tentative $\frac{3}{2}^+$ assignment was proposed by Beery, Kelley, and McHarris²³ and a definite assignment of $J = \frac{3}{2}$ was given in the level scheme proposed by Moreh and Nof.²⁶ The 9-keV separation of these two levels made it impossible to resolve them in the present experiment. Nevertheless, the angular distribution of the 1.125-MeV group (Fig. 6) provides useful information about each level. The absence of pronounced oscillations indicates that both levels are produced with comparable cross sections and that the two have opposite parity. Thus the 1.127-MeV level definitely has positive parity and only $J^\pi = \frac{3}{2}^+$ is consistent with the other data.

Levels at 1.30 and 1.65 MeV are populated with approximately equal strength via $l = 0$ transitions in the $^{140}\text{Ce}(^3\text{He}, d)^{141}\text{Pr}$ reaction.^{4,5} Therefore definite J^π assignments of $\frac{1}{2}^+$ were possible. It is difficult, however, to establish the correspondence between these two $\frac{1}{2}^+$ states and the levels at about 1.295 and 1.653 MeV indicated by our ex-

periments. This difficulty stems from the fact that closely spaced pairs of levels at 1.2925 and 1.2984 MeV and at 1.650 and 1.6572 MeV have been established by the higher-resolution γ -ray experiments. Wildenthal¹ has identified these $\frac{1}{2}^+$ states with the 1.2984- and 1.6572-MeV levels populated in the decay of ^{141}Nd .²³ The former identification seems quite certain, since a probable value of $\frac{5}{2}^+$ for the 1.2925-MeV level was obtained in the decay-scheme study.²³ On the other hand the identification of the 1.65-MeV $\frac{1}{2}^+$ state with the 1.657-MeV level is uncertain. We have identified

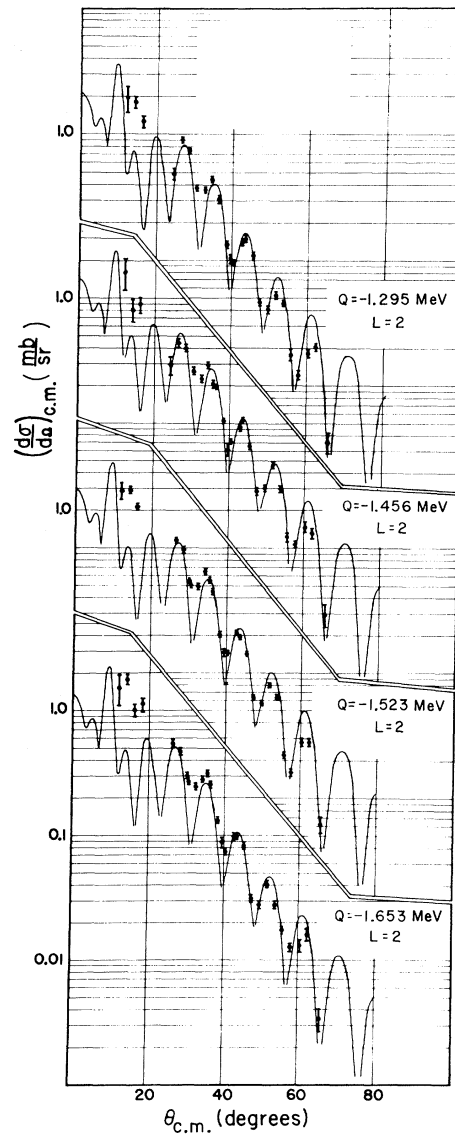


FIG. 5. Angular distributions for (α, α') transitions to positive-parity levels in the 1.29–1.66-MeV region. The solid curves are DWBA predictions for $L = 2$, with 102 P.W. and including Coulomb excitation. The partial deformation lengths (β_{LR}^p) are defined in the text.

(column 9, Table I) this upper $\frac{1}{2}^+$ state with the 1.650-MeV level simply on the basis of energy values. It is possible that all four levels are populated with appreciable strength in inelastic scattering, and, if so, positive parity is indicated for each of them.

The α -particle angular distribution for the composite group of levels between 1.76 and 1.85 MeV (Fig. 7) shows a lack of structure which suggests that both positive- and negative-parity states are present. With the 35-keV resolution of the present experiment, it was not possible to ascertain the parities of individual members of this group. However, it is important for the purpose of determining the active shell-model configurations to know that negative-parity states extend into this lower region of the excitation spectrum.

2. Negative-Parity Multiplet, 2.0–2.5 MeV

Eight levels were identified between 2.002 and 2.388 MeV in the present work. The levels at 2.368 and 2.388 MeV were not resolved in the

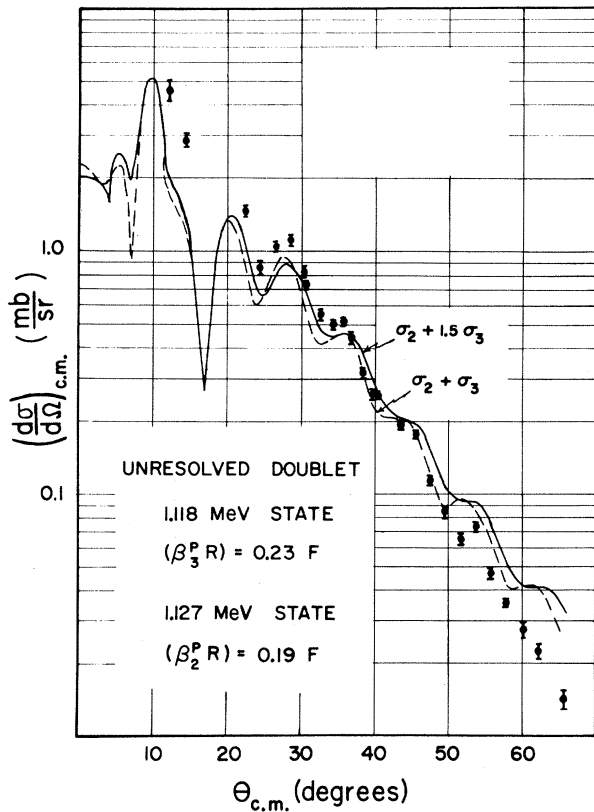


FIG. 6. The composite angular distribution for (α, α') transitions to the unresolved levels at 1.118 and 1.125 MeV. The solid curves represent mixtures of $L=2$ and $L=3$ DWBA predictions, in the proportions indicated in the figure. The reduced cross section σ_L and the partial deformation lengths $(\beta_L^P R)$ are defined in the text.

(α, α') spectra but appear as a noticeably broad peak. The excitation energies determined from the (d, d') spectrum correspond quite closely to the values reported by Ellegaard *et al.*,⁷ except for a level at 2.256 MeV which they did not observe. The peak corresponding to this level can be seen in the (d, d') spectrum of Fig. 2, but the corresponding group was clearly visible in the (α, α') spectra only at angles favoring positive parity. It does not appear in the (α, α') spectrum of Fig. 1, which was taken at an angle near a minimum in the positive-parity angular distributions. Another group was observed at 2.464 MeV in the (d, d') spectrum and in the (α, α') spectra at angles favoring negative-parity states. Since its position coincides with that of the octupole 3^- state in ^{140}Ce and a corresponding level was not observed in the (d, d') experiment of Ellegaard

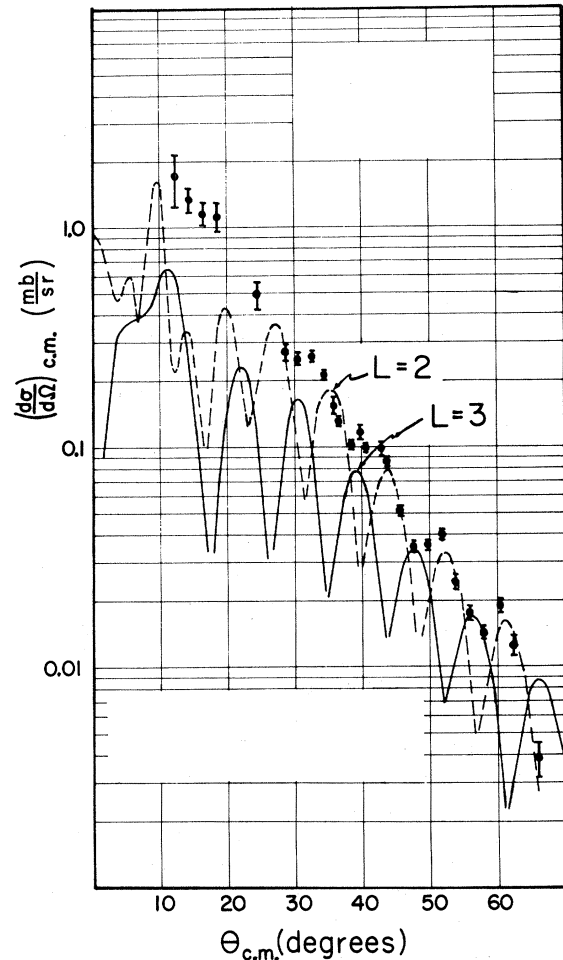


FIG. 7. The composite angular distribution for (α, α') transitions to the unresolved group of levels between 1.76 and 1.85 MeV. The absence of a well-structured oscillatory pattern indicates that both positive- and negative-parity levels are populated.

et al.,⁷ we attribute it to the presence of a small Ce impurity in the target. In addition to the eight levels discussed, the existence of four more levels in this region at 2.016, 2.235, 2.272, and 2.348 MeV is indicated by the (γ, γ') experiment of Moreh and Nof.²⁶

The angular distributions for inelastic α -particle scattering to all of the levels in this region, except that at 2.250 MeV, show odd- L character. However, none of the experiments provides a basis for determining unique spin values for these levels.

3. Levels Above 2.5 MeV

In the 170-keV region between 2.39 and 2.56 MeV there are no levels populated with appreciable strength in the (α, α') and (d, d') reactions. The only other experiment which examined this portion of the spectrum is the $^{141}\text{Pr}(\gamma, \gamma')$ experiment of Moreh and Nof.²⁶ Their results are consistent with an energy gap of 130 keV in this region. If this energy gap is real, it is probably the last one of this magnitude in the excitation spectrum of ^{141}Pr . Above 2.56 MeV the level density becomes dense indeed, as can be seen from Figs. 1 and 2. However, several α -particle groups were well enough resolved in the present experiment so that angular distributions could be obtained. These are shown in Figs. 8 and 9 and the parities deduced from these data are given in Table I.

The levels observed at 2.566 and 2.585 MeV by Ellegaard *et al.*⁷ probably correspond to the 2.57-MeV shoulder appearing at the right of the 2.609-MeV peak in the (d, d') and (α, α') spectra of Figs. 1 and 2. The remaining levels reported in Ref. 7 up to 2.930 MeV were also identified in the present (d, d') spectrum. An additional level at 2.730 MeV, not reported in Ref. 7, was identified in the (d, d') spectrum and appeared at some angles in the (α, α') spectra as an unresolved shoulder at the left of the 2.684-MeV peak.

The angular distributions for the α -particle groups appearing at 2.609, 2.684, and 2.986 MeV are shown in Fig. 8. The moderately well-structured angular distributions for the 2.609- and 2.986-MeV groups indicate that they arise predominantly from transitions to levels with even parity. The DWBA predictions for pure $L = 2$ transitions are shown with the data. The agreement with these predictions is qualitatively similar to that observed for transitions to the positive-parity states in the 1.2–1.7-MeV region and the deformation parameters (see Sec. IV B) are of comparable magnitude. In a study of the $^{140}\text{Ce}(\alpha, \alpha')$ reaction¹¹ an $L = 2$ transition was observed to a state at 2.90

MeV with a strength about equal to the total observed for the 2.609- and 2.986-MeV levels. Thus, it is not surprising to find moderately strong transitions to positive-parity states at about this energy in ^{141}Pr . The character of the angular distribution for the 2.684-MeV group is ambiguous, but it exhibits mild oscillations which are in phase with the $L = 3$ prediction shown with the data. It therefore seems likely that the major contribution to this group is a transition to a negative-parity state.

The angular distributions for additional α -particle groups which were observed at 2.876 and 3.135 MeV (Fig. 9) have almost no structure, suggesting

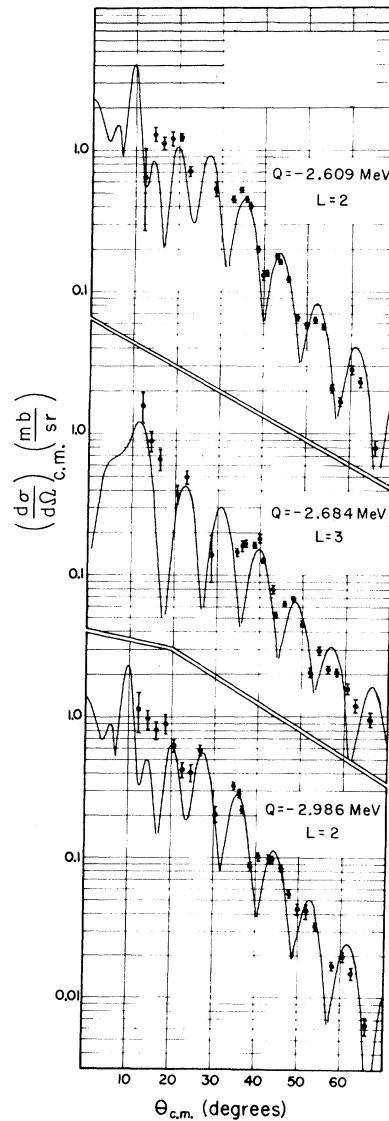


FIG. 8. Angular distributions for (α, α') transitions to levels in the 2.6–3.0-MeV region. The solid curves are DWBA predictions for $L = 2$ (2.609- and 2.986-MeV levels) and $L = 3$ (2.684-MeV level).

that they are due to transitions to unresolved levels having both positive and negative parity. Four more α -particle groups were observed between 3.2 and 3.6 MeV but the angular distributions were not determined. Many additional weakly populated levels are suggested by the rather high background in this energy range. The levels above 4.0 MeV were not studied because of the increasing level density and the interference from strong carbon and oxygen contaminant peaks.

B. Extraction of Spectroscopic Parameters

A summary of the spectroscopic parameters deduced from the present experiment is given in Table III. Also listed in the table are the corresponding values for the lowest 2^+ , 3^- , and 4^+ states in ^{140}Ce , based upon the results of a study of Baker and Tickle¹¹ of the $^{140}\text{Ce}(\alpha, \alpha')$ reaction. These were obtained from an analysis²⁷ which employed the same optical potential used in the analysis of the present ^{141}Pr experiment.

Since the 4^+ state at 2.08 MeV in ^{140}Ce is excited with moderate strength in the $^{140}\text{Ce}(\alpha, \alpha')$ reaction, it is probable that some of the even- L transitions observed to levels in ^{141}Pr contain $L = 4$ admixtures. However, reliable values for the $L = 4$ strength could not be determined from the data, and we have therefore parametrized the even- L transition strengths in terms of pure $L = 2$ transitions. The deformation parameters for these transitions were determined on the basis of a visual fit to the DWBA predictions which gave primary consideration to the four maxima between 25 and 55°. With this normalization the maximum at about 62° is lower than the DWBA calculation. We also note that the data at angles less than 20° are above the pure $L = 2$ predictions, which may indicate the presence of $L = 4$ admixtures. The first maximum predicted for an $L = 4$ transition is at 14°, and the first maximum for the $L = 4$ transition to the 2.08-MeV 4^+ state in ^{140}Ce is observed to occur at about that angle.¹¹ It is in this region that the even- L angular distributions, for example the four angular distributions shown in Fig. 5, deviate considerably from the predictions for $L = 2$. Unfortunately, however, the data in this angular range are insufficient, due to interference from carbon and oxygen contaminants, to establish with reliability the presence of $L = 4$ contributions to the cross sections. At larger angles, where the experimental angular distributions are well defined, the reduced cross sections $\sigma_2(\theta)$ and $\sigma_4(\theta)$ are nearly in phase, making it difficult to distinguish between the two possibilities.

Two types of uncertainties must be considered in extraction of deformation lengths from the mea-

sured angular distributions. First, there are uncertainties in the experimental cross sections in the angular range (25–60°) that was selected for the comparison with DWBA calculations. In effect these cross sections were determined by comparing inelastic yields with elastic yields (see Sec. II). This method removes all but (1) relative uncertainties in target thickness, solid angle, track counting, etc., (2) statistical uncertainties, and (3) uncertainties resulting from the DWBA analysis. The over-all uncertainty in (1) and (2), primarily due to track counting, is 10–15%, and the measured deformation lengths (Table III) have resultant uncertainties of 5–8% from these sources

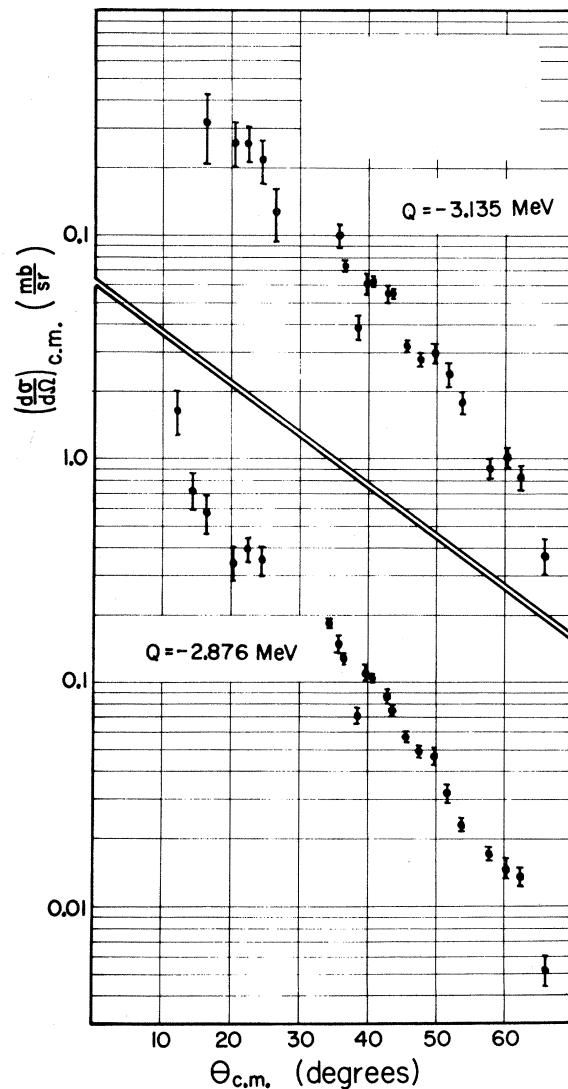


FIG. 9. Angular distributions of inelastic α -particle groups corresponding to $Q = -2.876$ MeV and $Q = -3.135$ MeV. The lack of structure in both angular distributions suggests that several levels with different parity are being populated.

(excluding the 1.118–1.127-MeV doublet to be discussed below). To study the sensitivity of the extracted deformation lengths to the parameters of the analysis, reduced cross sections were calculated with the four different potentials of Ref. 14. These give comparable fits to the elastic scattering but differ in the real well depths (consistent with the discrete ambiguity in α -particle potentials). With these potentials the calculated $L=2$ and 3 angular distributions are quite similar in the range $0-80^\circ$. The maximum difference in the deformation lengths that would have resulted from the use of any other of these potentials is approximately 8%. Thus the values given in Table III are quite insensitive to this ambiguity in the DWBA analysis.

The angular distribution for the two unresolved levels at about 1.12 MeV was analyzed as a composite of $L=2$ and $L=3$ transitions. The curves shown in Fig. 6 correspond to the combinations of reduced cross sections $\sigma_2 + 1.5\sigma_3$ (solid line) and $\sigma_2 + \sigma_3$ (dashed line). The deformation values given in Table III result from fitting the $\sigma_2 + 1.5\sigma_3$ combination to the data. The uncertainty in these quantities is quite large, since for the combination $\sigma_2 + w\sigma_3$ a rather large range of w values (1.0–1.8) gave acceptable fits to the composite angular distribution.

TABLE II. Center-of-mass differential cross sections divided by Rutherford cross sections for the elastic scattering of 45.0-MeV α particles on ^{141}Pr . The relative cross sections (σ/σ_R , given in exponential form) have been normalized to unity at 7.2° . The uncertainties given with each number reflect counting statistics only.

$\theta_{c.m.}$	σ/σ_R	$\theta_{c.m.}$	σ/σ_R
7.2	$\equiv 1$	42.9	$5.56 \pm 0.12 (-2)$
8.1	$9.47 \pm 0.03 (-1)$	45.0	$4.52 \pm 0.10 (-2)$
8.4	$9.75 \pm 0.04 (-1)$	47.0	$5.92 \pm 0.14 (-2)$
9.6	$9.54 \pm 0.05 (-1)$	49.0	$4.79 \pm 0.10 (-2)$
9.9	$9.41 \pm 0.05 (-1)$	51.1	$2.37 \pm 0.06 (-2)$
10.1	$9.56 \pm 0.05 (-1)$	53.1	$1.51 \pm 0.06 (-2)$
12.2	$1.126 \pm 0.011 (0)$	55.2	$2.26 \pm 0.11 (-2)$
14.2	$1.125 \pm 0.010 (0)$	57.2	$2.38 \pm 0.12 (-2)$
16.3	$1.137 \pm 0.019 (0)$	59.2	$1.47 \pm 0.08 (-2)$
18.3	$9.93 \pm 0.20 (-1)$	61.3	$6.28 \pm 0.62 (-3)$
20.4	$7.61 \pm 0.09 (-1)$	62.3	$5.38 \pm 0.40 (-3)$
22.5	$6.86 \pm 0.09 (-1)$	63.3	$6.78 \pm 0.44 (-3)$
24.5	$5.76 \pm 0.11 (-1)$	65.3	$1.07 \pm 0.08 (-2)$
26.6	$3.94 \pm 0.10 (-1)$	67.3	$8.75 \pm 0.58 (-3)$
28.6	$3.08 \pm 0.07 (-1)$	69.4	$4.40 \pm 0.25 (-3)$
30.7	$2.97 \pm 0.07 (-1)$	71.4	$2.15 \pm 0.22 (-3)$
32.7	$2.32 \pm 0.05 (-1)$	73.4	$3.68 \pm 0.36 (-3)$
34.8	$1.43 \pm 0.03 (-1)$	75.4	$4.37 \pm 0.44 (-3)$
36.8	$1.22 \pm 0.02 (-1)$	77.4	$2.50 \pm 0.25 (-3)$
38.8	$1.28 \pm 0.03 (-1)$	79.4	$9.1 \pm 1.1 (-4)$
40.9	$9.87 \pm 0.21 (-2)$		

The angular distributions for the multiplet of seven levels at 2.002, 2.078, 2.106, 2.178, 2.320, 2.368, and 2.388 MeV are shown in Fig. 10. Only the composite angular distributions were obtained for the 2.078–2.106-MeV and 2.368–2.388-MeV doublets. It can be seen from the figure that all the angular distributions have regular oscillations in phase with the elastic scattering angular distribution. Therefore, the assignment of negative parity to these levels is quite certain. It is likely that they are excited by nearly pure $L=3$ transitions, since the 2.46-MeV 3^- state is the only negative-parity level below 3 MeV which is excited with appreciable strength in the $^{140}\text{Ce}(\alpha, \alpha')$ reaction.¹¹ The curves displayed in the figure correspond to DWBA predictions for pure $L=3$ transitions. The deformation parameters were determined on the basis of a visual fit to the four

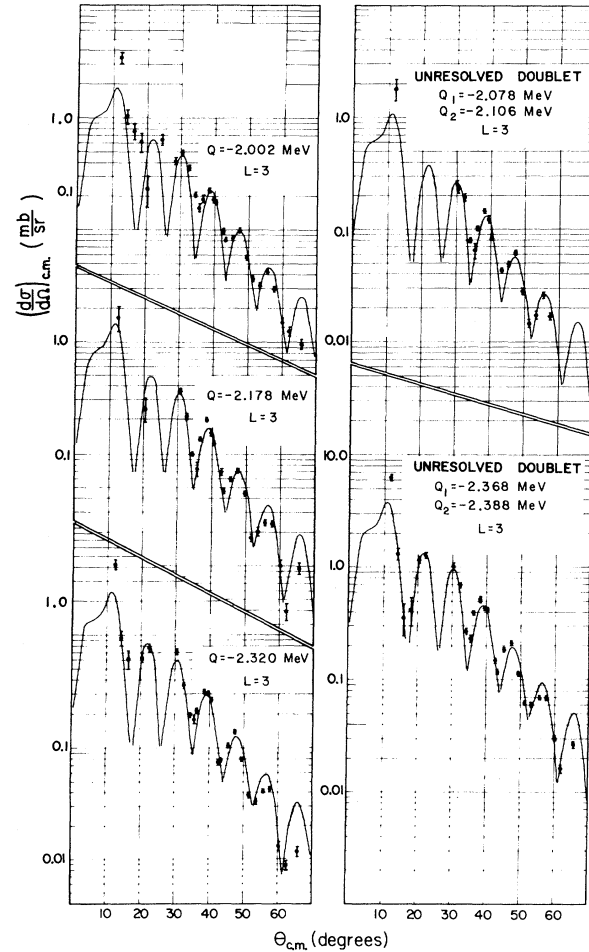


FIG. 10. Angular distributions for (α, α') transitions to negative-parity levels in the 2.0–2.4-MeV region. The solid curves are DWBA predictions for $L=3$, with 80 P.W. and including Coulomb excitation. The partial deformation lengths ($\beta_L^2 R$) are defined in the text.

maxima between 28 and 60°. The use of this procedure results in a poor fit to the data between 60 and 70°. The agreement at angles less than 25° is fairly good, although the data at 12° are always above the calculated curves.

For the sake of completeness we have estimated electromagnetic transition strengths G_L in Weisskopf single-particle units, based upon the transition strengths $(\beta_L R)^2$ determined from the inelastic

TABLE III. Summary of spectroscopic information deduced from the present experiment. Energy and J^π values for ^{141}Pr are taken from the collation of results presented in Table I. The values of β_L^2 determined by Baker and Tickle for the lowest 2^+ , 4^+ , and 3^- states of ^{140}Ce are shown for comparison. The estimated electromagnetic transition probabilities G_L in Weisskopf single-particle units were computed with the formula given in the text.

	E_x (MeV)	J^π	Assumed L value	$10^4 \times \beta_L^2$	$(\beta R)^a$ (F)	G_L
^{140}Ce	1.597	2^+	2	45	0.49	8.3
	2.084	4^+	4	29	0.40	6.0
	2.464	3^-	3	82	0.66	5.5
^{141}Pr	0.145	$\frac{7}{2}^+$	2	$\leq 2^b$	≤ 0.06	≤ 0.1
	1.118	$\frac{11}{2}^-$	3	9.9	0.23	1.9
	1.127	$\frac{3}{2}^+$	2	6.6	0.19	1.3
	1.293	$\frac{5}{2}^+$	2	7.4 ^c	0.20	1.4
	1.298	$\frac{1}{2}^+$	2			
	1.456	$+$	2	5.0	0.16	0.9
	1.521	$(\frac{3}{2})^+$	2	10.3	0.23	1.9
	1.650	$\frac{1}{2}^+$	2	4.8	0.16	0.9
	2.003	$-$	3	9.1	0.22	1.8
	2.079	$-$	3	5.4 ^c	0.17	1.1
	2.107	$-$	3			
	2.177	$-$	3	7.0	0.19	1.3
	2.320	$-$	3	12.0	0.25	2.3
	2.368	$-$	3	19.5 ^c	0.32	3.7
	2.388	$-$	3			
2.608	$+$	2	8.5	0.21	1.6	
2.681	$-$	3	6.5	0.19	1.3	
2.986	$+$	2	5.0	0.16	0.9	
^{141}Pr	$\sum_J [\beta_J^P(J)]^2 = 47.6^d$		$\sum_J [\beta_J^P(J)]^2 = 69.4$			

^aOver-all uncertainties are approximately 10% for ^{141}Pr (see Sec. IV B).

^bBased on upper limit of intensity in α -particle spectrum at 40°.

^cUnresolved doublet in α -particle spectra.

^dThe 0.145-MeV level was not included in the sum.

scattering. These are given in Table III. With the exception of the 0.145-MeV first excited state (for which a value of $\beta_L R$ could not be determined in the present experiment) the electromagnetic transition rates for levels in ^{141}Pr are not known; hence a direct comparison with our estimates is not possible. Nonetheless the values of G_L extracted from the present data provide a guide to the transition rates to be expected. They were obtained from the relation^{28, 29}

$$G_L = \frac{Z^2 (L+3)^2 (\beta_L R)^2}{4\pi (2L+1) 1.2A^{1/3}}. \quad (10)$$

Equation (10) depends upon the assumption that the transition is collective and that the deformation length $\beta_L R$ is the same for both nuclear and electromagnetic transitions. Also, a spherical uniform charge density of radius $1.2A^{1/3}$ is assumed. It is known³⁰ that the latter assumption underestimates the contribution of the charge density in the nuclear-surface region. However, for the present purpose we have not included the relatively small correction³⁰ for this.

It is possible to use the present data to estimate the lifetime of the $\frac{11}{2}^-$ state at 1.118 MeV. For this level we estimate $G_3 = 1.9$ W.u., which corresponds to a transition probability $\lambda(E3) = 2.8 \times 10^6 \text{ sec}^{-1}$ for decay to the ground state. Dave, Nelson, and Wilenzick²⁵ found that the 1.118-MeV level decays to the 0.145-MeV first excited state and to the ground state with relative intensities of 0.9 and 0.1, respectively. If we take our estimate of G_3 to represent 10% of the total γ -ray width for the 1.118-MeV level, we obtain for it a mean lifetime of 36 nsec. Although the uncertainty in this estimate is rather large, it seems likely that the lifetime of the 1.118-MeV level would be accessible to measurement by electronic techniques. Observation of the delayed 0.973-MeV γ ray following reactions such as $^{141}\text{Pr}(\alpha, \alpha'\gamma)$ or $^{139}\text{La}(\alpha, 2m\gamma)$ appears to be a possible method for measuring this lifetime.

C. Comparison with Predictions of the Weak-Coupling Model

On the basis of the weak-coupling model, levels in ^{141}Pr strongly excited by inelastic scattering would be the members of the particle-vibration multiplets arising from the coupling of the $2d_{5/2}$ one-quasiparticle (1-qp) ground state of ^{141}Pr with vibrational excitations of the ^{140}Ce core. Taking as the most important core excitations the first 2^+ and 3^- states, one would have a positive-parity quintuplet of the form $|2^+ \times 2d_{5/2}; J^+\rangle$ with $J = \frac{1}{2}, \frac{3}{2}, \frac{5}{2}, \frac{7}{2},$ and $\frac{9}{2}$, and a septuplet of negative-parity levels $|3^- \times 2d_{5/2}; J^-\rangle$ with spins ranging from $\frac{1}{2}$ to

$\frac{1}{2}$. According to the model the members of each multiplet would be excited with cross sections proportional to $(2J+1)$. However, one expects to observe only an approximate correspondence with these simple expectations. The $|2^+ \times 2d_{5/2}; J\rangle$ and $|3^- \times 2d_{5/2}; J\rangle$ multiplets are close in energy to similar configurations based upon the $1g_{7/2}$ 1-qp state (which in ^{141}Pr is only 145 keV from the $2d_{5/2}$ 1-qp level), as well as to other levels resulting from additional core excitations present in the same energy range. Thus we expect considerable mixing to occur. Nevertheless it is of interest to investigate, in the light of spin and parity information from other experiments, the degree of validity retained by the simple model.

At approximately the position of the 1.597-MeV 2^+ state of ^{140}Ce , a group of five strong transitions to positive-parity levels at 1.127, 1.295, 1.456, 1.523, and 1.653 MeV is observed in the present experiment. These have measured $[\beta_2^P]^2$ values (in units of 10^{-4}) of 6.6, 7.4, 5.0, 10.3, and 4.8, respectively. Taking the condition $\sum[\beta_2^P]^2(^{141}\text{Pr}) = \beta_2^2(^{140}\text{Ce}) = 45$, the weak-coupling model predicts for the five members of the $|2^+ \times 2d_{5/2}; J^+\rangle$ multiplet $[\beta_2^P]^2 = 3.0, 6.0, 9.0, 12.0, \text{ and } 15.0$, in order of increasing spin. The relative intensities measured for the five transitions do not resemble very closely these model expectations, and the sum of the measured $[\beta_2^P]^2$ values is 34.1 compared with the model prediction 45.0. Also the center of gravity of the observed levels is approximately 200 keV below the position of the 2^+ state in ^{140}Ce .

The 1.653-MeV level has the smallest measured value of $[\beta_2^P]^2$, and might therefore be considered a leading candidate for a $\frac{1}{2}^+$ assignment. It was pointed out in Sec. IV A that $\frac{1}{2}^+$ states are known to exist at 1.30 and 1.65 MeV, but that the identification with our 1.295- and 1.653-MeV levels is uncertain, since at each energy there are two levels separated by approximately 5 keV. On the other hand, if it is true that the observed splitting of the $l=0$ strength in the $^{140}\text{Ce}(^3\text{He}, d)^{141}\text{Pr}$ reaction is due to mixing of the $|2^+ \times 2d_{5/2}; \frac{1}{2}^+\rangle$ particle-vibration state with the $3s_{1/2}$ 1-qp state, one would expect both of the $\frac{1}{2}^+$ levels observed in the $(^3\text{He}, d)$ reaction to be populated in inelastic scattering through their particle-vibration components. The sum of the $[\beta_2^P]^2$ values measured for the 1.295- and 1.653-MeV transitions is considerably greater than the weak-coupling prediction for the $\frac{1}{2}^+$ particle-vibration state, which suggests that at least some of the strength observed for these transitions is due to unresolved levels having other particle-vibration components. In particular, the 1.295-MeV transition may include contributions from both the 1.2925-MeV ($\frac{5}{2}^+$) and 1.2984-MeV ($\frac{3}{2}^+$) levels, with the 1.2925-MeV level carrying a signifi-

cant fraction of the $|2^+ \times 2d_{5/2}; \frac{5}{2}^+\rangle$ strength.

The most likely candidate for a $|2^+ \times 2d_{5/2}; \frac{3}{2}^+\rangle$ assignment is the level at 1.1268 MeV, which is known to have $J^\pi = \frac{3}{2}^+$. This level was not resolved in the present experiments, but it was possible to obtain a value of the deformation parameter for it, using the procedure discussed in Sec. IV B. Although the value we obtain ($[\beta_2^P]^2 = 6.6$) is rather uncertain, it fits in nicely with the weak-coupling prediction of $[\beta_2^P]^2 = 6.0$ for the $\frac{3}{2}^+$ member of the particle-vibration multiplet. Moreover it is interesting to note that the 1.1268-MeV level was not observed in the proton-transfer reactions, while another $\frac{3}{2}^+$ level at 1.60 MeV, which carried all the $2d_{3/2}$ strength observed in the $^{140}\text{Ce}(^3\text{He}, d)^{141}\text{Pr}$ reaction, is not excited with appreciable strength by inelastic scattering. Thus the experiments indicate that there is little interaction between the $\frac{3}{2}^+$ particle-vibration state and the $2d_{3/2}$ 1-qp state.

The 1.523-MeV level has the largest measured deformation parameter ($[\beta_2^P]^2 = 10.3$), suggesting that it has a large value of J . This level was not observed in the $^{141}\text{Pr}(\gamma, \gamma')$ experiment,²⁶ which is expected to populate (via dipole γ -ray transitions from a $\frac{5}{2}^-$ resonance level) levels with $J = \frac{3}{2}, \frac{5}{2}, \text{ and } \frac{7}{2}$. Nor was it populated in the decay²³ of ^{141}Nd . Since the ground state of ^{141}Nd has $J^\pi = \frac{3}{2}^+$, allowed transitions in electron-capture decay would populate only states in ^{141}Pr having $J^\pi = \frac{1}{2}^+, \frac{3}{2}^+, \text{ or } \frac{5}{2}^+$. The fact that the 1.523-MeV level was not observed in these two experiments, together with the evidence from the present experiment, would suggest a value of $\frac{9}{2}^+$ for the 1.523-MeV level.

The remaining strong positive-parity transition observed in the 1.2–1.7-MeV region is to the level at 1.456 MeV. Although it is by default the only candidate for the $\frac{7}{2}^+$ member of the particle-vibration multiplet, the value $[\beta_2^P]^2 = 5.0$ measured for this level is well under the weak-coupling expectation of 12.0. However one can construct many other $\frac{7}{2}^+$ configurations in the same region of excitation, and it may be that these lead to considerable fragmentation of the transition strength. One weak piece of evidence consistent with a $\frac{7}{2}^+$ assignment is that Moreh and Nof²⁶ have suggested a J^π value of either $\frac{3}{2}^+$ or $\frac{7}{2}^+$ for a level at 1.451 MeV. It is possible that this level corresponds to the “1.456-MeV” level populated in the present experiments.

The negative-parity septuplet would be expected near the position of the 3^- state in ^{140}Ce , which is at 2.46 MeV. As was the case for the positive-parity multiplet, the results of the present experiment are only approximately in accord with weak-coupling-model expectations. Including the $\frac{1}{2}^-$ state at 1.118 MeV and assuming the presence of at least one negative-parity level in the cluster of levels near 1.8 MeV (see Sec. IV A1), a minimum

of 10 negative-parity levels are populated with appreciable strength. These mostly lie between 2.0 and 2.4 MeV. The levels for which $[\beta_3^P]^2$ could be obtained have a total $\sum[\beta_3^P]^2 = 69.4$, compared with the value $\beta_3^2 = 82$ measured³⁰ for the 3^- state of ^{140}Ce .

The observed proliferation of negative-parity levels and the downward shift from the position of the octupole state may in part be due to the presence of additional negative-parity configurations based on the coupling of the $2d_{5/2}$ and $1g_{7/2}$ 1-qp states with the 2.350-MeV 5^- state of ^{140}Ce . An additional possibility, the mixing of the $|3^- \times 2d_{5/2}; \frac{11}{2}^- \rangle$ state with the $1h_{11/2}$ 1-qp state, is suggested by experiment. The 1.118-MeV $\frac{11}{2}^-$ state is populated strongly in both the $^{140}\text{Ce}(^3\text{He}, d)^{141}\text{Pr}$ reaction^{1,4} and the present inelastic scattering experiment, indicating that this level has significant particle-vibration and $1h_{11/2}$ 1-qp components. The value of $[\beta_3^P]^2$ we obtain for the 1.118-MeV level is approximately 40% of the weak-coupling estimate ($[\beta_3^P]^2 = 23.4$) for the $\frac{11}{2}^-$ member of the $|3^- \times 2d_{5/2}; J^- \rangle$ multiplet, based on the value of β_3^2 measured³⁰ for the 3^- state of ^{140}Ce . If one assumes that this level is adequately described by the wave function

$$a|3^- \times 2d_{5/2}; \frac{11}{2}^- \rangle + b|1h_{11/2} \rangle,$$

the orthogonal state

$$b|3^- \times 2d_{5/2}; \frac{11}{2}^- \rangle - a|1h_{11/2} \rangle$$

is expected to lie somewhere below 3 MeV. It is therefore quite likely that one of the seven negative-parity levels observed in the 2.0–2.4 MeV region is the other $\frac{11}{2}^-$ state. Since this state should be populated by $l = 5$ transfer in the $^{140}\text{Ce}(^3\text{He}, d)^{141}\text{Pr}$ reaction, but has not been observed, it would be interesting to search for it.

D. Comparison with Shell-Model Predictions

The positive-parity level structure of $N = 82$ nuclei has been the subject of two recent shell-model treatments.^{1,2} The experimental excitation spectrum of ^{141}Pr is compared with the predictions of the two calculations in Fig. 11. The experimental energies, spins, and parities were taken from column 9 of Table I.

The most striking features of the measured ^{141}Pr spectrum are that (1) two nearly degenerate levels with spin-parity values $\frac{5}{2}^+$ and $\frac{7}{2}^+$ are lowest in energy; (2) there is a relatively large energy gap of approximately 1 MeV between these two levels and the next group of levels; (3) there is a large number of levels (≈ 20) in the region between 1 and 2 MeV, most of which have positive parity; (4) most

of the levels between 2.0 and 2.5 MeV which are observed in the $^{141}\text{Pr}(\alpha, \alpha')$ reaction have negative parity; and (5) the density of levels is exceedingly high above 2.5 MeV. A shell-model calculation must reproduce these qualitative features if it is to provide some understanding of the nuclear structure. In addition it is important that the calculation predict reasonably well the electromagnetic transition probabilities and spectroscopic factors deduced from reaction experiments.

In a calculation performed by Wildenthal¹ the residual surface- δ interaction (SDI) was diagonalized in a large positive-parity vector space based on a closed $Z = 50$, $N = 82$ core. Included were all configurations with nine protons in the $1g_{7/2}$ and $2d_{5/2}$ orbits, and all configurations having eight protons distributed in these two orbits with the additional proton in either the $2d_{3/2}$ or $3s_{1/2}$ orbit. The relevant single-particle energies and the residual-force parameter were determined by fitting the calculated energies of selected levels in $N = 82$ nuclei (excluding ^{141}Pr) to experimental values.

It can be seen in Fig. 11 that the qualitative features of the positive-parity spectrum are reproduced quite well by the calculation. In the range between 1- and 2-MeV excitation, the model predicts 25 positive-parity levels with spins ranging from $\frac{1}{2}$ to $\frac{17}{2}$. The various experiments indicate the existence of 19 established levels in this region (excluding the $\frac{11}{2}^-$ 1.118-MeV level), and four additional tentative levels. This total includes the multiplet at 1.75–1.85-MeV, which according to the argument given in Sec. IV A apparently contains at least one level with negative parity. However there remain approximately 20 levels, with either undetermined parity or known positive parity, which have been observed between 1 and 2 MeV. Excluding from the predicted levels those with spins of $\frac{13}{2}$, $\frac{15}{2}$, and $\frac{17}{2}$, one is left with just 20 levels. Since it is probable that levels with such high spins would not have been detected by the experiments, the number of levels predicted in the 1–2-MeV region is in quite good agreement with the presently available experimental information.

Other positive-parity levels are predicted above 2 MeV. Since most of the observed levels in this region have negative parity, a comparison with the model predictions is not possible. However, at this excitation energy we expect the assumptions of the model to begin to break down. For example, one expects configurations not included in the calculations, such as $(1h_{11/2})^2$, to have an effect upon the positive-parity levels.

The complexity of the many-component wave functions which result from the diagonalization of large shell-model matrices often makes it difficult to discern the structural features of the states

which they describe. For example, the 39 states predicted by the calculation of Wildenthal can be classified readily only by excitation energy and the quantum numbers J and π . Further insight into the nature of these states is provided by the coupling scheme of Hecht and Adler.² These authors have shown that for mixed configurations of identical nucleons it is possible to classify eigenstates of the SDI by the pseudospin and pseudo-orbital angular momentum quantum numbers B and C . The first of these plays the role of a generalized seniority quantum number, specifying the number of energetically unfavored $J \neq 0$ pairs. In an application of the new scheme to the $(g_{7/2}-d_{5/2})^n$ system,² they have also shown that to a good approximation the SDI can be replaced by a generalized pairing interaction (GPI) for which the energy eigenvalues can be written in the closed form

$$E = -G \frac{2c+1}{2c+3} \left[\frac{1}{4}(n-v)(4c+4-n-v) - B(B+1) + \frac{3}{4}n + \frac{1}{4}n(n-1) \right], \quad (11)$$

where G is the force-strength parameter and v is the total seniority. For states of the $(g_{7/2}-d_{5/2})^n$ system c has the value 3, and if n is odd B assumes values of $\frac{1}{2}, \frac{3}{2}, \dots, \frac{n}{2}$. In the GPI approximation, the excitation energies of the system depend only upon v, B , and the value chosen for G . When n is odd they are given by

$$E(v, B) - E(v=1, B=\frac{1}{2}) = G \frac{2c+1}{2c+3} \left[B(B+1) + (v-1)(c+1) - \frac{1}{4}(v^2+2) \right]. \quad (12)$$

The spectrum given by this expression, with $G = 0.343$ MeV, is shown at the right in Fig. 11. For

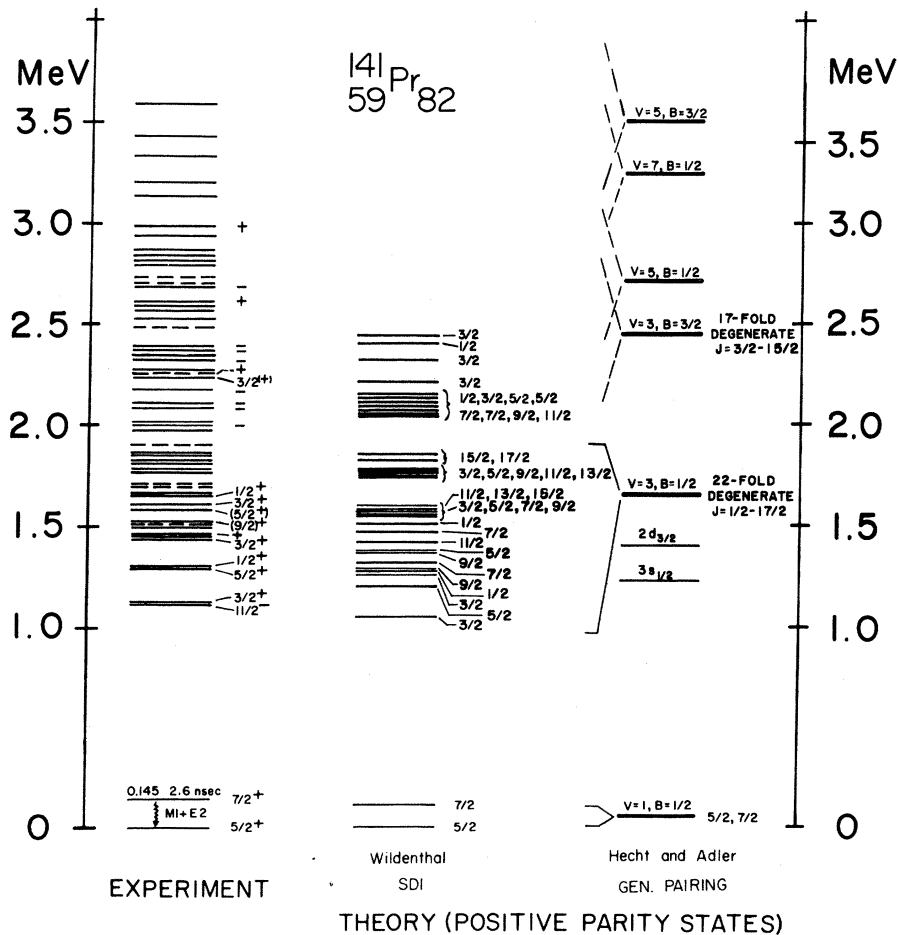


FIG. 11. Comparison of the experimentally observed spectrum of ^{141}Pr with shell-model predictions discussed in the text. The experimental results are a combination of all the measurements summarized in Table I. The dashed levels are uncertain.

completeness we have also included the $2d_{3/2}$ and $3s_{1/2}$ 1-qp states in the 1.0–1.5-MeV region.

It is interesting to note that a rather sizable energy separation (0.8 MeV) is predicted between $B = \frac{1}{2}$ and $B = \frac{3}{2}$ states having total seniority $\nu = 3$. For our choice of G the 22-fold degenerate $B = \frac{1}{2}$ and 17-fold degenerate $B = \frac{3}{2}$ multiplets lie at 1.65 and 2.45 MeV, respectively. When the GPI is replaced by the SDI, the degeneracy of the $B = \frac{1}{2}$ levels (but not of the $B = \frac{3}{2}$ multiplet) is removed.² However, the energy splittings are small (≤ 0.1 MeV). When the energy separation of the $1g_{7/2}$ and $2d_{5/2}$ shell-model orbits is taken into account, the degeneracy of all multiplets is removed through the single-particle part of the Hamiltonian. This term also causes mixing of the $B = \frac{1}{2}$ and $B = \frac{3}{2}$ states with $\nu = 3$. (Its matrix elements are subject to the selection rules $|\Delta B| \leq 1, |\Delta C| \leq 1$). Nevertheless, the dominant components of states in the 1–2-MeV region are expected³¹ to have $\nu = 3, B = \frac{1}{2}$, while the states in the 2.0–2.5-MeV region are expected to have mostly $\nu = 3, B = \frac{3}{2}$.

The GPI predictions and the predictions of the exact SDI calculation by Wildenthal are nearly identical so far as the total number of levels and the number of occurrences of the same J value in the 1.0–2.5-MeV region are concerned. Thus both treatments give the same qualitative agreement with the presently known spectrum of ^{141}Pr , and the more detailed comparison made earlier with the calculation of Wildenthal applies also to the description given by Hecht and Adler.

Hecht and Adler have also pointed out that under certain assumptions their coupling scheme leads to a selection rule for inelastic scattering.² They have shown that only $\Delta B = 0$ transitions have non-zero matrix elements, provided, for a given multipole component of the projectile-nucleon interaction, one can neglect the variation in the radial integrals between different single-particle states of the target. Baker²⁷ has investigated the validity of this assumption for the $^{140}\text{Ce}(\alpha, \alpha')$ reaction and finds it to be quite well justified. This is due to the dominance of the contributions to the reaction from the external region of the nucleus, where the form factors based on $1g_{7/2}$ and $2d_{5/2}$ single-particle states are quite similar. The results of the present experiment are in qualitative agreement with the $\Delta B = 0$ selection rule. Since the ground state of ^{141}Pr presumably has $\nu = 1$ and $B = \frac{1}{2}$, transitions to the many $\nu = 3, B = \frac{1}{2}$ states in the 1–2-MeV region are allowed, and many such transitions are observed. On the other hand, the positive-parity levels in the 2.0–2.5-MeV region are expected³¹ to be predominantly $B = \frac{3}{2}$ in character and the $\Delta B = 1$ transitions to these levels are forbidden by the model. It is interesting to note that although many

levels in the latter region are observed in the present experiment, all have negative parity with the exception of the weakly populated level at 2.256 MeV. While two additional positive-parity levels were identified at 2.609 and 2.986 MeV, most of the numerous positive-parity levels which surely exist above 2 MeV in the spectrum of ^{141}Pr are not excited with appreciable strength in the (α, α') reaction. If the 2.609- and 2.986-MeV levels have pure $\nu = 3, B = \frac{3}{2}$ configurations (and the ground state has pure $\nu = 1, B = \frac{1}{2}$), the transitions to these levels would imply a breakdown of the $\Delta B = 0$ selection rule. Alternatively they may have $\nu = 3, B = \frac{1}{2}$, although this would indicate an unexpectedly large energy spread in the $B = \frac{1}{2}$ states. The most likely explanation³¹ for these transitions is that they are due to mixing between the $\nu = 3$ states with $B = \frac{1}{2}$ and $B = \frac{3}{2}$, and possibly some $\nu = 3, B = \frac{3}{2}$ admixtures in the ground state, and that they reflect this mixed character while preserving the $\Delta B = 0$ selection rule.

V. SUMMARY

The 35-keV resolution obtained in the present (α, α') experiments was found to be insufficient to resolve many closely spaced levels in the 1–3-MeV excitation spectrum of ^{141}Pr . Therefore a detailed level-by-level analysis of our results was precluded. However, the major features of the collective excitations were found to be a group of at least five strongly excited positive-parity levels between 1.12 and 1.65 MeV, a group of at least seven negative-parity levels between 2.00 and 2.39 MeV, appreciable transition intensity to levels as high as 3.5 MeV, and a significant collective component for the $\frac{1}{2}^-$ state at 1.118 MeV. The following conclusions can be reached. First, a simple weak-coupling model based upon the 2^+ and 3^- core states and the $2d_{5/2}$ 1-qp state cannot explain the number of levels and transition strengths observed in the (α, α') reaction. An extended basis, including additional core excitations and/or mixing with states based on the $1g_{7/2}$ 1-qp state would be required. Second, the general features of transitions to even-parity states in the 1–2-MeV region are consistent with the shell-model calculations of Wildenthal¹ and Hecht and Adler.² The transitions to positive-parity states above 2 MeV were not expected on the basis of a simple interpretation of the $\Delta B = 0$ selection rule.² These transitions probably imply³¹ some mixing between $B = \frac{1}{2}$ and $B = \frac{3}{2}$ states.

ACKNOWLEDGMENTS

We thank F. T. Baker and C. Ellegaard for communicating results prior to publication. Numerous

discussions with K. T. Hecht and F. T. Baker were most helpful. We are grateful to P. D. Kunz for supplying the distorted-wave code DWUCK and to the University of Colorado Nuclear Physics Laboratory for support of one of us (H.W.B.) during

the completion of the distorted-wave calculations and the preparation of the manuscript. Finally, we thank W. E. Downer and the cyclotron operating staff for their assistance in this work.

*Work supported in part by the U. S. Atomic Energy Commission.

†Present address: Nuclear Physics Laboratory, University of Colorado, Boulder, Colorado 80302.

¹B. H. Wildenthal, *Phys. Rev. Letters* **22**, 1118 (1969), and *Phys. Letters* **29B**, 274 (1969).

²K. T. Hecht and A. Adler, *Nucl. Phys.* **A137**, 129 (1969).

³W. P. Jones, L. W. Borgman, J. Bardwick, and W. C. Parkinson, to be published.

⁴W. P. Jones, dissertation, University of Michigan, 1969 (unpublished); L. W. Borgman, dissertation, University of Michigan, 1969 (unpublished).

⁵B. H. Wildenthal, E. Newman, and R. L. Auble, *Phys. Letters* **27B**, 628 (1968); E. Newman, K. S. Toth, R. L. Auble, R. M. Gaedke, and M. F. Roche, *Phys. Rev. C* **1**, 1118 (1970); B. H. Wildenthal, R. L. Auble, E. Newman, and J. A. Nolen, *Bull. Am. Phys. Soc.* **13**, 1430 (1968); E. Newman, R. L. Auble, and B. H. Wildenthal, *ibid.* **14**, 56 (1969); B. H. Wildenthal, E. Newman, and R. L. Auble, *ibid.* **14**, 1239 (1969).

⁶W. P. Jones, L. W. Borgman, W. C. Parkinson, and J. Bardwick, *Bull. Am. Phys. Soc.* **12**, 1189 (1967); L. W. Borgman, W. P. Jones, and J. Bardwick, *ibid.* **13**, 658 (1968); L. W. Borgman, W. P. Jones, J. Bardwick, and W. C. Parkinson, *ibid.* **14**, 491 (1969); W. P. Jones, L. W. Borgman, J. Bardwick, and W. C. Parkinson, *ibid.* **14**, 491 (1969).

⁷C. Ellegaard, G. Samosvat, P. Vedelsby, and K. Jorgensen, *Bull. Am. Phys. Soc.* **14**, 492 (1969), and private communication.

⁸H. W. Baer and J. Bardwick, *Nucl. Phys.* **A129**, 1 (1969).

⁹O. Hansen, O. Nathan, L. Vistisen, and R. Chapman, *Nucl. Phys.* **A113**, 75 (1968).

¹⁰O. Hansen and O. Nathan, *Nucl. Phys.* **42**, 197 (1963).

¹¹F. T. Baker and R. S. Tickle, *Bull. Am. Phys. Soc.* **14**, 1219 (1969), and *Phys. Letters* **32B**, 47 (1970).

¹²S. Ofer and A. Schwarzschild, *Phys. Rev.* **116**, 725 (1959).

¹³H. W. Baer, J. J. Reidy, and M. L. Wiedenbeck, *Nucl. Phys.* **A113**, 33 (1968).

¹⁴D. F. Jackson and C. G. Morgan, *Phys. Rev.* **175**, 1402 (1968).

¹⁵W. C. Parkinson and R. S. Tickle, *Nucl. Instr. Methods* **18**, 19, 93 (1962).

¹⁶L. McFadden and G. R. Satchler, *Nucl. Phys.* **84**, 117 (1966).

¹⁷D. F. Jackson and V. K. Kumbhavi, *Phys. Rev.* **178**, 1626 (1969); C. G. Morgan and D. F. Jackson, *Phys. Rev.* **188**, 1758 (1969).

¹⁸R. H. Bassel, G. R. Satchler, R. M. Drisko, and E. Rost, *Phys. Rev.* **128**, 2693 (1962).

¹⁹E. Rost, *Phys. Rev.* **128**, 2708 (1962).

²⁰J. S. Blair, *Phys. Rev.* **115**, 928 (1959).

²¹G. R. Satchler, in *Lectures in Theoretical Physics*, edited by P. D. Kunz and W. E. Brittin (University of Colorado Press, Boulder, Colorado, 1966), Vol. VIII C, pp. 134-136.

²²P. D. Kunz, private communication.

²³D. B. Beery, W. H. Kelley, and Wm. C. McHarris, *Phys. Rev.* **171**, 1283 (1968).

²⁴P. van der Merwe, I. J. van Heerden, W. R. McMurray, and J. G. Malan, *Nucl. Phys.* **A124**, 433 (1969).

²⁵V. R. Dave, J. A. Nelson, and R. M. Wilenzick, *Nucl. Phys.* **A142**, 619 (1970).

²⁶R. Moreh and A. Nof, *Phys. Rev.* **178**, 1961 (1969).

²⁷F. T. Baker, private communication.

²⁸I. M. Naqib and J. S. Blair, *Phys. Rev.* **165**, 1250 (1968).

²⁹A. M. Bernstein, in *Advances in Nuclear Physics*, edited by M. Baranger and E. Vogt (Plenum Press, Inc., New York, 1970), Vol. III, pp. 325-476.

³⁰L. W. Owen and G. R. Satchler, *Nucl. Phys.* **51**, 155 (1964).

³¹K. T. Hecht, private communication.